13 Computer Assisted Physics

C. Bersier, T. Mayer, P. F. Meier, S. Renold, E. Stoll, and A. Uldry
guests: T. A. Claxton and M. Eremin

13.1 Effects of strong correlations on the spin susceptibility

in collaboration with: M. Eremin, Kazan State University and I. Eremin, Freie Universitt Berlin

Up to now calculations of the spin susceptibility for cuprates were performed in the framework of weak–coupling approximations. However, it is known that cuprates belong to Mott–Hubbard doped materials where electron correlations are important. We have investigated the effect of strong correlations on high–T_c superconductors. In particular, we have derived an analytic expression for the spin susceptibility below T_c which results for a model system that is closely related to models based on the idea of the formation of copper–oxygen singlets in layered cuprates. Then we numerically ev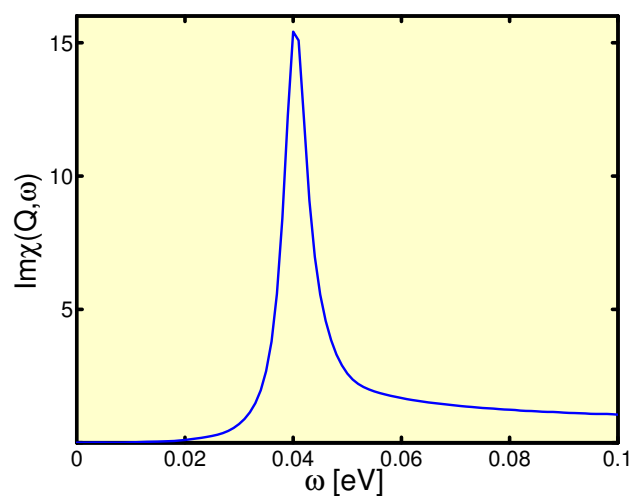aluated the expression of the susceptibility using parameter values adopted to measurements of the Fermi surface, neutron scattering and NMR data. In Fig. 13.1 the energy dependence of the imaginary part of the calculated susceptibility at the antiferromagnetic wave vector $\mathbf{Q}$ is shown. We observe a large peak near the frequency $\omega \simeq 41$ meV, as observed in neutron scattering measurements. Using the same parameter values we studied the temperature dependence of various NMR properties in the superconducting state including Knight shifts, spin–spin relaxation and spin–lattice relaxation times. Part of this work is published in Ref. (1).


Figure 13.1:
Imaginary part of the susceptibility at the antiferromagnetic wave vector $\mathbf{Q}$.

[1] T. Mayer, M. Eremin, I. Eremin and P. F. Meier, Physica C, **408-410**, 400 (2004).

13.2 Suppression of critical properties in doped cuprates

In high-T_c superconductors dopant atoms supply holes or excess electrons. Electric conduction occurs in the neighborhood of dopants within a circle in the CuO_2 - plane that is several

Figure 13.2:
Calculated temperature dependence of the specific heat of $La_{2-x}Sr_xCuO_4$ for Sr concentrations $x = 0.00179$ (crosses), 0.00367 (+ signs), 0.00776 (circles), 0.0124 (triangles up), and 0.0239 (triangles down). The thin full lines are guides for the eyes. The relative uncertainties due to statistical fluctuations of the in-homogeneities and the Monte Carlo processes are of the order of 3% at each point. The remaining antiferromagnetic lattice has a size of 302×302 sites (lattice constant a), covered with non magnetic discs of a diameter of 6.04 a. Arrows denote the effective Néel temperatures. The red full line corresponds to the exact specific heat of the pure system; the violet dashed, dashed-dotted, and dotted lines have been calculated for a pure $32 \times \infty$, $16 \times \infty$, and an $8 \times \infty$ lattice [2]. The blue dashed double-dotted line corresponds to calculations [3] of a system of 64×64 sites.
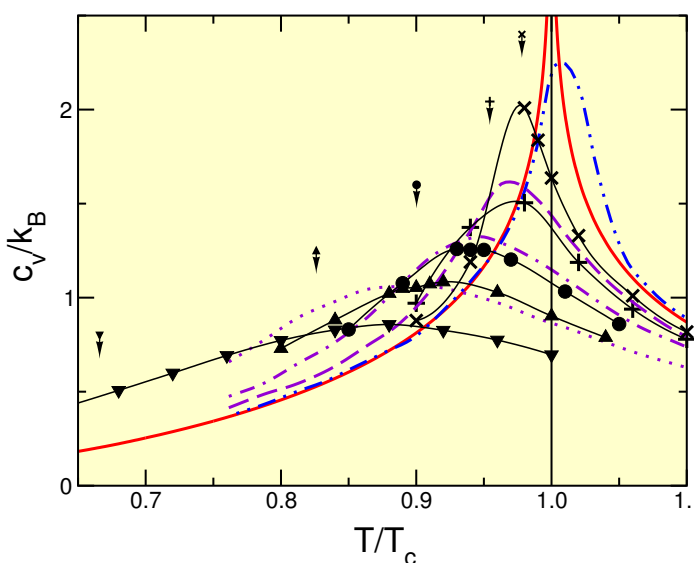
lattice constants wide. Percolation of these conducting areas then leads to global conduction. Diffusing d-electrons in these areas can destroy antiferromagnetism. It has been shown (1) that in $La_{2-x}Sr_xCuO_4$ high-T_c superconductors the Néel temperatures decrease with increasing doping even when the systems are simulated with Ising instead of Heisenberg interactions. A system close to the magnetic percolation limit exhibits isolated small clusters responsible for the observed spin glass behavior at low temperatures. The simulations of the specific heat show that the singularities which occur in infinite pure systems, vanish for finite doped systems. It is expected that for infinitely large doped systems the peak heights increase with system sizes, however, the small grain sizes of the cuprates (4) stop such an increase, so that the peak heights decrease and the peak widths grow with doping in these materials (see Fig. 13.2). A similar behavior is also visible for the staggered susceptibility χ and the antiferromagnetic correlation length. Such a growth of the peak widths has also been observed in nuclear quadrupole resonance spectra of doped superconducting $La_{2-x}Sr_xCuO_4$ (5), in contrast to the very narrow peaks of the pure antiferromagnetic insulating La_2CuO_4 (6).

[1] E. P. Stoll, J. Phys. A, **38**, 125 (2005).

[2] Helen Au-Yang and Michael. E. Fisher, Phys. Rev. B, **11**, 3469 (1975).

[3] Arthur E. Ferdinand and Michael. E. Fisher, Phys. Rev., **185**, 832 (1969).

[4] T. Schneider, Journal of Superconductivity: Incorporating Novel Magnetism, **17**, 41 (2004).

[5] Y.-Q Song, M. A. Kennard, M. Lee, K. R. Poppelmeier, and W. P. Halperin, Phys. Rev. B, **44**, 7159 (1991).

[6] T. Imai, C. P. Slichter, K. Yoshimura, and K. Kosuge, Phys. Rev. Lett., **70**, 1002 (1993).

13.3   Charge and spin density distributions around Zn impurities in cuprates

In hole doped cuprates non-magnetic impurities like Zn and others are detrimental (1) and superconductivity disappears with a few percent of Zn dopants. It is well known that the doping of the cuprates by holes destroys the antiferromagnetic correlations. In contrast, it has been proposed that Zn doping enhances antiferromagnetic correlations (2; 3). Abrikosov (4) following recent numerical calculations of Kaplan *et al.* (5), proposed that Zn, creating an excess positive charge at the copper site, reduces the hole concentration in its vicinity.
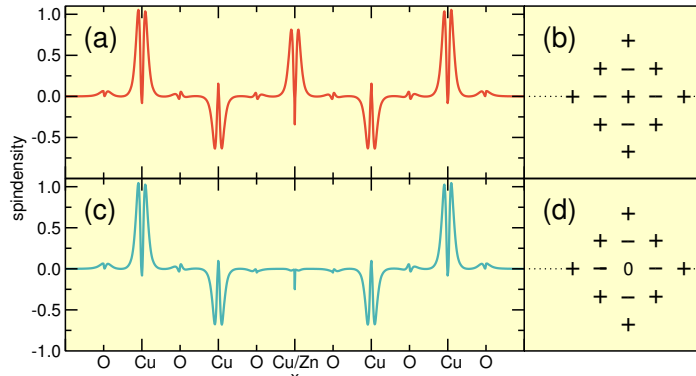

Figure 13.3:
(a) Spin density along the 5 Cu and 6 O in the $Cu_{13}O_{62}/Cu_{12}La_{66}$ Cu cluster with spin multiplicity M=6; (c) spin density with Zn substitution and multiplicity M=5.

We have investigated the effect of zinc substitution on the local electronic structure of several cuprates using first-principles cluster calculations. Clusters comprising until 13 copper atoms in the cuprate plane of La_2CuO_4, $YBa_2Cu_3O_7$, and $YBa_2Cu_4O_8$ were used.

We illustrate the antiferromagnetic spin arrangement with the $Cu_{13}O_{62}/Cu_{12}La_{66}$ cluster for La_2CuO_4. We performed calculations by choosing a spin multiplicity of $M = 6$. In Fig. 13.3a the spin density along the Cu-O bonds in the plane is displayed for an undoped Cu_{13} cluster. In the right panel (Fig. 13.3b) the signs of the Mulliken spin densities at the planar Cu sites are shown which exhibit an antiferromagnetic spin arrangement, with adjacent copper sites having opposite spins. Near the copper, most of the spin density is provided by a singly occupied $3d_{x^2-y^2}$ atomic orbital (AO). Its square has maxima at distances of 0.345 Å from the nucleus but vanishes at the nucleus where the spin densities are provided by s orbitals.

The two copper atoms at the outermost right and left positions in Fig. 13.3a have only one NN copper ion whereas the one in the center has four NN with negative spin densities and the two remaining coppers have four NN with positive spin densities. These differences allow the determination of on-site and transferred hyperfine fields as has been demonstrated in Refs. (6; 7). Near the oxygens, the spin density is provided by the $2p_x$ AO and the contact density is very small for antiferromagnetically arranged copper neighbors.

The introduction of zinc at the cluster center introduces an extra electron into the cluster and it is to be noted that the spin state of lowest energy is now the $M = 5$ state with a corresponding spin density along the Cu-O bonds that is shown in the lower panel of Fig. 13.3c. This leaves the antiferromagnetic arrangement virtually intact although there is a detectable reduction in the spin density on the coppers which are nearest neighbors to the zinc perhaps due to a slight delocalization of the electron of opposite spin on the zinc (see Fig. 13.3c). The Mulliken spin density on the Zn is practically zero, as to be expected (Fig. 13.3d).

The results show that the effects of Zn substitution are rather local as concerns the electronic structure. The charge content on the oxygens surrounding Zn is lower than in the pure compound which we interpret as destroying superconductivity locally in the vicinity of Zn.

We were also able to calculate electric field gradients (EFG) at the Cu sites and compared them to experiment. We find that the EFG values for the nearest neighbor coppers to Zn are larger than in the undoped compounds whereas those of the next nearest neighbors (NNN) are smaller. We also showed that for a Cu nucleus adjacent to a Zn the spin-lattice relaxation rate would be considerably reduced which is not what is observed experimentally. With these two arguments we conclude that the experimentally observed ^{63}Cu satellite peak with lower NQR frequency probably originates from copper nuclei that are NNN to Zn.

[1] G. Xiao, M. Z. Cieplak, J. Q. Xiao, and C. L. Chien, Phys. Rev. B, **42**, 8752 (1990).

[2] M.-H. Julien, T. Fehér, M. Horvatić, C. Berthier, O. N. Bakharev, P. Ségransan, G. Collin, and J.-F. Marucco, Phys. Rev. Lett., **84**, 3422 (2000).

[3] Y. Itoh, T. Machi, C. Kasai, S. Adachi, N. Watanabe, N. Koshizuka, and M. Murakami, Phys. Rev. B, **67**, 064516 (2003).

[4] A. A. Abrikosov, Physica C, **397**, 77 (2003).

[5] I. G. Kaplan, J. Soullard, and J. Hernández-Cobos, Phys. Rev. B, **65**, 214509 (2002).

[6] P. Hüsser, H. U. Suter, E. P. Stoll, and P. F. Meier, Phys. Rev. B, **61**, 1567 (2000).

[7] S. Renold, S. Pliberšek, E. P. Stoll, T. A. Claxton, and P. F. Meier, Eur. Phys. J. B, **23**, 3 (2001).

13.4   Re-assessment of NMR data in the cuprates

The traditional approach to interpreting NMR spin-lattice relaxation rates in the cuprates has been originally developed in 1990 by Millis, Monien and Pines and is generally known as the MMP theory (1). This method is able to model the different temperature dependence of the planar copper and oxygen relaxation rates by identifying two contributions to the spin susceptibility. One is strongly peaked at the antiferromagnetic wave vector and dominates the copper relaxation rate. The other, associated to a Fermi liquid contribution, is essentially wave vector independent and is responsible for the oxygen relaxation. The procedure suffers however from the following drawback: the hyperfine fields are added coherently at the copper site but incoherently at the oxygen site. We put forward a model in which such a distinction needs not be made *a priori*. Rather, the degree of coherency is determined from the value of the correlations between electronic copper spins. Furthermore, no assumption is made from the start on the form of the susceptibility or to what contributes to it.

We come back to a well established expression for the spin-lattice relaxation rate of a nucleus k, $^{k}T_{1\alpha}^{-1} = {}^{k}U_{\beta} + {}^{k}U_{\gamma}$, when a field is applied in the crystallographic direction α. The relaxation is caused by fluctuating fields $^{k}U_{\beta}$ and $^{k}U_{\gamma}$ in the directions perpendicular to the applied field. When the relaxation rates are known experimentally in the different directions, the contributions $^{k}U_{\alpha}$ can be easily computed. It turns out that the temperature dependence of all $^{k}U_{\alpha}$ is similar ($^{k}U_{\alpha}$ is growing with increasing temperature), and there is no contrasting temperature difference between the copper and the oxygen contributions.

Using a simple model of fluctuating fields (2), we obtained that $^{k}U_{\alpha}(T) = {}^{k}V_{\alpha}(T)\,\tau_{eff}(T)$. $\tau_{eff}(T)$ is an effective correlation time, and the $^{k}V_{\alpha}$ in the copper-oxide plane are expressions in terms of the hyperfine field constants and static spin-spin correlations. Typically for the oxygen, $^{17}V_{\alpha} \propto (1 + K_{01}^{\alpha})$, where the nearest neighbor antiferromagnetic spin correlation $K_{01}^{\alpha} = 4\langle S_0^{\alpha} S_1^{\alpha}\rangle$ varies between -1 and 0 in function of the temperature. The field at the copper site is given by the on-site contribution, plus the transfered fields from the 4 nearest

neighbors, so that the expression $^{63}V_\alpha$ for copper contains also next-nearest neighbor and next-next-nearest neighbor correlations. In the limit of a fully antiferromagnetic system, $^{63}V_\alpha$ is simply given by the coherent addition of hyperfine field constants $(A_\alpha - 4B)^2$, whereas in the limit of no correlations, they are incoherently added as $(A_\alpha^2 + 4B^2)$. The spin correlations provide the interpolation between those extremes in function of the temperature.

In order to make the model numerically tractable, we assumed that the higher order correlations depend on K_{01}^α and decrease exponentially with the distance between spins. By computing the *ratios* of relaxation rates, including those between different nuclei, the τ_{eff} cancel out by assumption. In the case of YBa$_2$Cu$_3$O$_7$, where the whole range of data for copper, oxygen and yttrium are available, we were able to fit the hyperfine field constants and determine $K_{01}^\alpha(T)$ between 100 K and 300 K. Using those values we went back to the data and extracted τ_{eff}, which could be extremely well fitted with the function $\tau_{eff}^{-1} = \tau_1^{-1} + \tau_2^{-1}$, where $\tau_1 \propto T$ and τ_2 constant. The linear dependence of τ_{eff} at low temperature hints at a relaxation process dominated by scattering of quasi-particles in a Fermi liquid. At high temperature, $\tau_{eff} \to \tau_2$. In order to determine what dominates the relaxation there, we examined the copper spin relaxation data available for the La$_{2-x}$Sr$_x$CuO$_4$ series. As the rates for all dopings, including that of the insulating parent compound, converge to the same constant value at high temperature, we concluded that τ_2 can be associated to the fluctuations of local spins in a paramagnet.

The validity of the model and the fitting formula for τ_{eff} could be convincingly tested by confronting our high temperature predictions with high temperature relaxation rates data in YBa$_2$Cu$_3$O$_7$. We analyzed then the underdoped compounds of the YBaCuO series. In particular, some very precise measurements of the copper relaxation rate are available for the YBa$_2$Cu$_4$O$_8$ compound. A whole fit could not be done in this substance, since only measurements along the c-axis were made. However, taking the same correlations and hyperfine field constants found in YBa$_2$Cu$_3$O$_7$, we can determine τ_{eff} between 100 K and 300 K and fit it with $\tau_{eff}^{-1} = \tau_1^{-1} + \tau_2^{-1}$. This time however, τ_1 is not linear but goes like $\tau_1 \propto Te^{-g/T}$, where g is a further adjustable parameter. The result for the reconstructed relaxation rate is shown in Fig. 13.4, along with the data used for the fit (crosses) and further high temperature data.

Our prediction (solid line) is in striking agreement with the experiment.

In summary, we proposed a way of looking at the spin-lattice relaxation data which is adapted to the anisotropic nature of the cuprate materials. The degree of coherency of the
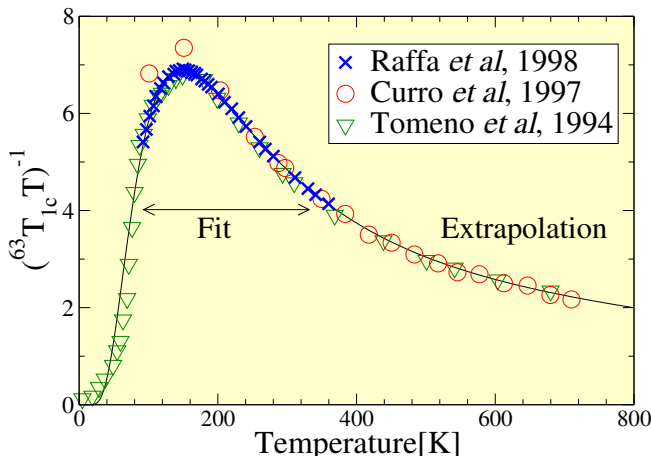

Figure 13.4:
NQR data from Raffa *et al.* **[3] for YBa$_2$Cu$_4$O$_8$ and fit as in the text (solid line), and comparison with data from Curro** *et al.* **[4] and Tomeno** *et al.* **[5].**

hyperfine fields is the same at all time for all nuclei, but varies with the temperature in function of the antiferromagnetic spin-spin correlations. The success of the predictions at high temperature confirms the validity of the model, which we believe could help identifying the underlying physical processes in the cuprates.

[1] A. J. Millis, H. Monien and D. Pines, J. Phys.: Condens. Matter, **42**, 167 (1990).

[2] **Principles of magnetic resonance**, C. P. Slichter, Springer, Berlin, 1996.

[3] F. Raffa, T. Ohno, M. Mali, J. Roos, D. Brinkmann, K. Conder and M. Eremin,
     Phys. Rev. Lett., **81**, 5912 (1998).

[4] N. J. Curro, T. Imai, C. P. Slichter and B. Dabrowski, Phys. Rev. B, **56** , 877 (1997).

[5] I. Tomeno, T. Machi, K. Tai, N. Koshizuka, S. Kambe, A. Hayashi, Y. Ueda and H. Yasuoka,
     Phys. Rev. B, **49** , 15327 (1994).